ACS Photonics

pubs.acs.org/journal/apchd5

Letter

Multilayer Fabrication of a Rainbow of Microdisk Laser Particles Across a 500 nm Bandwidth

Paul H. Dannenberg,[‖] Andreas C. Liapis,[‖] Nicola Martino, Jisoo Kang, Yue Wu, Anokhi Kashiparekh, and Seok-Hyun Yun*

Cite This: *ACS Photonics* 2021, 8, 1301−1306

Read Online

ACCESS | Metrics & More | Article Recommendations | Supporting Information

ABSTRACT: Laser particles are an emerging technology with unique stimulated emission properties. The ability to produce laser particles over a wide spectral range is critical for massive wavelength-division multiplexing. Here we show a novel method to fabricate semiconductor microdisk laser particles with emission wavelengths spanning 500 nm from a single epitaxial wafer. The wafer consists of nine gain layers of InGaAsP with different quaternary compositions to cover lasing wavelengths from 1150 to 1650 nm. With optical pumping at 1064 nm, these particles are then used to track the movements of thousands of individual cells in vitro.

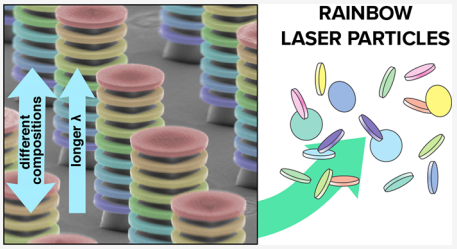

KEYWORDS: *cavities, lasers, nanoparticles, labeling, cell tracking, microdisks*

Micro- and nanolasers have been developed for use in various fundamental and applied sciences, including photonic circuits[1−3] and label-free biosensors.[4−10] While traditionally fabricated as on-chip devices,[11−14] the recent development of freestanding micro- and nanolasers, known as laser particles (LPs), has opened new avenues for utilizing lasers, particularly in cellular applications. Compared to the conventional luminescent particles used in biological applications, such as quantum dots and fluorescent beads, the most unique characteristic of LPs is their narrowband emission via lasing. This property has been harnessed to enable spectrally multiplexed single-cell barcoding.[15−17]

A variety of LPs have been developed using organic and inorganic materials in different forms.[15−21] Direct bandgap monocrystalline semiconductors, such as III−Vs, are a promising candidate for LP materials due to their high quantum efficiency, excellent photostability, and large refractive index. These materials are typically grown as layers on the surface of a parent substrate wafer using methods such as molecular beam epitaxy or metal organic chemical vapor deposition (MOCVD). Resonator structures, such as microdisk lasers, can then be defined from these layers by conventional lithography techniques and released into an aqueous environment by wet chemical etching of the underlying substrate.[17,21,22] This technique, however, suffers from two significant drawbacks. First, the production throughput of LPs by top-down lithography is generally lower than from chemical synthetic methods in which particles are produced in a reaction vessel from a three-dimensional volume of precursor materials. Second, to achieve broad spectral coverage of LP emission, multiple material compositions are usually required. For example, we have recently produced microdisk-type LPs covering the spectral range 1150−1550 nm from eptiaxially grown III−V semiconductor wafers using standard lithography and reactive-ion etching.[17] To achieve this broad spectral multiplexing, LPs from several different parent wafers, each with a different quaternary composition, needed to be combined (Figure 1a). This need for multiple separate fabrications complicates the process and makes the production of semiconductor LPs time-consuming and expensive.

In this work, we present a technique to parallelize the production of LPs over a wide spectral range. We devise a vertically stacked, multilayer epitaxial structure comprising a gradient of quaternary compositions. Multilayer, stacked heterostructures have previously been used to form lasers including the widely used vertical cavity surface emitting laser (VCSEL).[23] Lasing from vertically layered cavities made of III−V heterostructures has also been demonstrated in the context of studying mode-splitting phenomena in coupled cavities.[24,25] Furthermore, multiple III-nitride quantum wells of different compositions have been layered in a semiconductor microlaser to demonstrate simultaneous multicolor lasing from a single resonator.[26] However, unlike these studies in which multiple layers act in concert to form a single laser device on a chip, the active materials of our multilayer structure are designed to lase independently. Each resultant LP arises from a single gain material, and is separated from others to be released

Received: March 5, 2021
Published: April 28, 2021

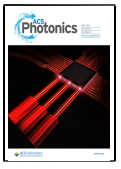

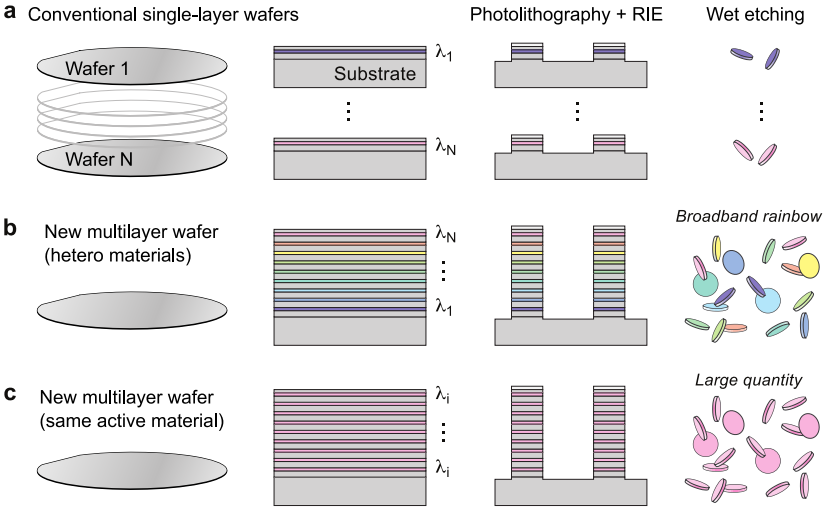

Figure 1. Schematic of the production process of disk-laser particles. (a) Conventional single-layer process where laser particles from many different wafers are combined. (b) Our simplified multilayer process. LPs with wavelengths spanning 500 nm are produced in a single shot from a single wafer. (c) Alternatively, a multilayer wafer where every layer has the same composition can be used to produce LPs in large quantities (approximately 1.3 billion per 3" wafer).

directly into an aqueous suspension. This allows us to simultaneously produce a rainbow of LPs spanning 500 nm from a single parent wafer (Figure 1b). Alternatively, by using a multilayer wafer where each layer has the same composition, we can produce LPs in large quantities (Figure 1c). Approximately 1.3 billion lasers can be produced from a single 3-in. wafer.

To demonstrate the usefulness of this technique, we track the movements of 5000 HeLa cells over 24 h.

RESULTS

Indium gallium arsenide phosphide ($In_{1-x}Ga_xAs_yP_{1-y}$), a direct-bandgap III−V semiconductor, can be lattice-matched to indium phosphide (InP) for $x = 0.1896y/(0.417 - 0.0158y)$.[27] Therefore, it is possible to grow a thick stack of multiple, alternating InGaAsP active and InP sacrifical layers on an InP substrate at typical rates of 1−2 μm/h using MOCVD.[28,29] As a quaternary compound, its optical gain can be tuned over a wide wavelength range by varying x and y, the relative quantities of Ga and As atoms, during the crystal growth process. For example, the stochiometric composition $In_{0.79}Ga_{0.21}As_{0.46}P_{0.54}$ has a bandgap of 1.03 eV, corresponding to a free-space wavelength of approximately 1200 nm whereas the smaller bandgap of $In_{0.59}Ga_{0.41}As_{0.88}P_{0.12}$, 0.80 eV, corresponds to a longer 1550 nm wavelength. To produce LPs with wavelengths spanning the 500 nm spectral window 1150−1650 nm (rainbow LPs), we designed an epitaxial semiconductor wafer structure (Figure S1) consisting of nine distinct 200 nm thick layers of $In_{1-x}Ga_xAs_yP_{1-y}$ with increasing As concentration from bottom to top while also increasing Ga concentration to enable each composition to remain lattice-matched to the InP substrate. This allowed the photoluminescence peak wavelength of each layer to be tuned at approximately 50 nm intervals. These InGaAsP layers were interspersed with 300 nm thick layers of InP and capped by a 200 nm InP layer. This multilayered, multicolored structure was produced by MOCVD in a single growth run.

A schematic illustrating the subsequent production of LPs from this structure is shown in Figure 1b, and experimental results are shown in Figure 2. A 2 μm thick layer of photoresist

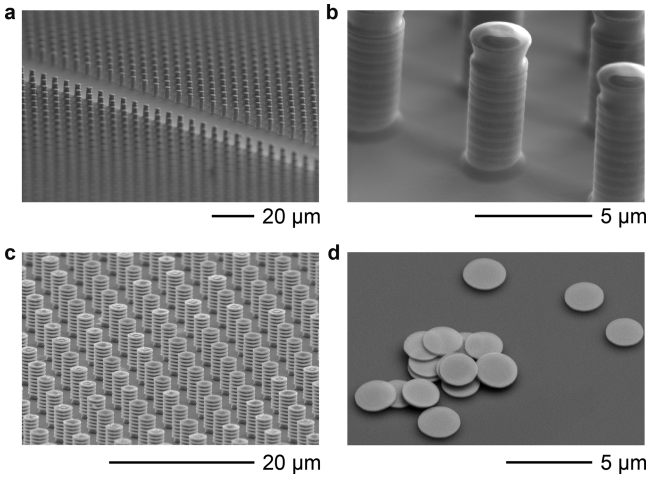

Figure 2. Scanning electron micrographs of (a, b) etched columns showing stacks of microdisk LPs, (c) columns after partial wet etching of the InP spacer layers, and (d) a collection of LPs that have been detached from their parent wafer.

(SU-8 2002) was spun onto the wafer surface and exposed by i-line UV light at 80 mJ/cm^2 through an opaque mask with a hexagonal array of transparent circles of nominal diameters 2.3, 2.4, 2.5, and 2.6 μm with an array spacing of 6 μm (Figure S2). Natural variations in the lithographic process result in a continuum of disk diameters. Following development, the pattern was transferred to the semiconductor by a highly anisotropic inductively coupled plasma reactive ion etching process (Plasmalab 100, Oxford Instruments) using hydrogen bromide chemistry, resulting in ∼7 μm tall columns (Figure 2b). The remaining SU-8 was then stripped using a two-round cleaning process consisting of, first, a dry plasma cleaning using a mixture of CF_4 and O_2, followed by a 30 s dip in room-temperature 1:1 H_2SO_4/H_2O, and a second plasma treatment using pure O_2 (Matrix 105), followed by another dip in the H_2SO_4 solution. For harvesting disks, the wafer was submerged in 3:1 HCl/H_2O under ultrasonication for 60 s. This acid etch corrodes the 300 nm sacrificial InP layers, resulting in the formation of rainbow InGaAsP microdisks in aqueous solution

https://doi.org/10.1021/acsphotonics.1c00343
ACS Photonics 2021, 8, 1301−1306

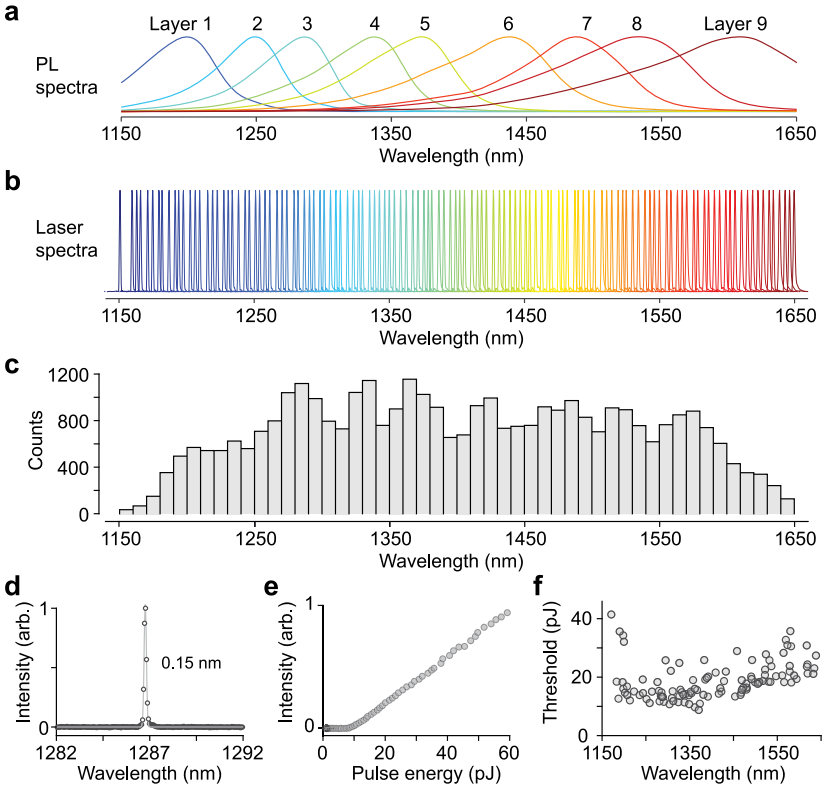

Figure 3. (a) Photoluminescence spectra of each of the nine layers in the multilayer wafer. (b) 126 lasing spectra of LPs spanning 500 nm. (c) Histogram of lasing wavelengths of 35830 LPs fabricated via our single-shot method. (d) Representative high-resolution spectrum showing above-threshold emission from an individual LP. (e) Representative input-output curve showing threshold behavior of an individual LP. (f) Variation of lasing threshold with lasing wavelength for a rainbow of LPs. LP diameters were between 2.1 and 2.4 μm.

(Figure 2d). HCl has a high etching selectivity to InP.[30] Therefore, the InGaAsP layers are largely unharmed after wet etching. The agglomeration of adjacent disks during the wet etch process was avoided by ultrasonic agitation (Figure S3). This method results in a yield of greater than 2×10^7 LPs per square cm of starting wafer.

The LPs were transferred into aqueous solution by neutralizing the HCl with NH_4OH, followed by washing in deionized water using four rounds of centrifugation and supernatant aspiration. Following this, the LPs were suspended in Matrigel (50% v/v), a curable gelatin matrix of refractive index 1.34 that mimics the properties of the cellular environment. The LP-encapsulating gel was mounted on a modified confocal microscope to measure the optical properties of the LPs. Using low, subthreshold-power continuous-wave 561 nm laser excitation, we identified nine distinct fluorescence spectra, corresponding to the nine InGaAsP compositions, showing a nearly regular spacing in the center wavelength as designed (Figure 3a). The width of the photoluminescence spectrum generally increases with increasing wavelength, that is to say, the width remains approximately constant in terms of optical frequency.

To characterize lasing spectra, we used a 1064 nm pump laser (spot size 2 μm, 10 ns pulse width, 2 MHz repetition rate), and analyzed the light emitted by each LP with a grating-based spectrometer equipped with a high-speed InGaAs linescan camera. The setup's spectral resolution could be varied between ~0.1 nm and ~1 nm depending on the chosen grating. With the 1 nm resolution grating, the spectrometer covers the spectral range of 1150 to 1650 nm. When pumped above threshold, the LPs each emit into a single lasing mode with a narrow line width, with wavelengths covering the entire spectral range (Figure 3b). Scanning the pump laser across a 3 mm × 3 mm × 0.1 mm volume of LP-filled Matrigel, we measured more than 35000 LPs and found a reasonably uniform distribution of single-mode emission wavelengths over the 500 nm spectral range (Figure 3c). The broad distribution across a continuum of wavelengths clearly demonstrates the effectiveness of our fabrication strategy combining different active materials, a photomask with several circle diameters, and the inherent variations in lithography and etching processes. Theoretical modeling of the resonant modes of a passive microdisk cavity suggests that the observed lasing arises from the eighth-14th order TE whispering gallery modes in the 1150−1650 nm range (Figure S4). For LPs originating from the same layer, variations in resonator size lead to variations in lasing wavelength within the roughly 100 nm gain bandwidth of the semiconductor. For disk diameters at which multiple resonant modes are supported, competition for gain between the modes usually dictates which one ultimately lases. As a rule of thumb, a 2 nm change in disk diameter results in ~1 nm difference in the lasing wavelength. Combining LPs with nine different semiconductor compositions in a single experiment allows us to cover a 500 nm bandwidth. Since cavities from all layers are in the same size range (2.1−2.4 μm); LPs originating from layers higher up in the stack (i.e., longer wavelength) operate at lower WGM orders.

Figure 3d,e shows a typical narrowband output spectrum and input−output curve from a single LP. Figure 3f shows the measured threshold pump energies for different LPs, which were calculated by determining the total amount of energy delivered to the disk per pump pulse by the focused pump

https://doi.org/10.1021/acsphotonics.1c00343
ACS Photonics 2021, 8, 1301−1306

laser. Despite the differences in material composition, wavelength, and diameter, each LP could be brought to threshold at a roughly similar pump energy (19 ± 6 pJ), as the threshold is mainly determined by the energy required to drive the semiconductor to transparency.[31] The slight increase in average threshold toward longer wavelengths likely stems from the uniform thickness (200 nm) of LPs, which decreases the effective refractive index of the cavity modes, thus, leading to a slightly lower radiative cavity Q factor. The high thresholds of a few LPs at short wavelengths may be due to the increased surface damage of the cavity material during the HCl wet etch transfer (Figure S5). LPs lasing at these wavelengths are comprised of $In_{1-x}Ga_xAs_yP_{1-y}$ compositions with smaller x and y and, therefore, share a greater degree of similarity to InP, which is known to be etched by HCl. Therefore, while any composition of $In_{1-x}Ga_xAs_yP_{1-y}$ spanning from InP (x, y = 0) to $In_{0.53}Ga_{0.47}As$ (x = 0.47, y = 1) can be incorporated into the InP lattice matched multilayer design, compositions with approximately y < 0.6 may be damaged during extensive HCl wet etching. At long wavelengths, the bandgap (≈1650 nm) of InGaAs offers a rough limit to the theoretical maximum lasing wavelength.

To enhance wavelength stability and biocompatibility, we coated the rainbow LPs with a 150 nm thick layer of silica using a Stöber growth chemistry[17] (Figure S6). Then, an in vitro culture of HeLa cells was incubated with silica-coated LPs for 48 h. Numerous mammalian cell types[17,21] have been shown to spontaneously uptake microdisk LPs in an endocytotic process,[32] which can be controlled via functional surface coating.[33] However, even with only a silica coating, about 70% of the HeLa cells internalized at least one LP, and the average number of LPs per cell was about 2. To identify the location of each LP, the modified confocal microscope simultaneously scanned both the low-power 561 nm CW laser beam for brightfield imaging and the 1064 nm pump laser across the culture dish. At each location, the transmitted intensity of the 561 nm laser was measured using a photomultiplier tube to generate a transmission image (Figure 4a). At the same time, LP emission spectra were recorded

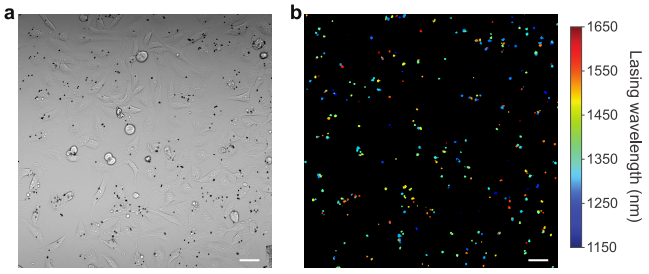

Figure 4. (a) LPs inside HeLa cells. (b) Spectral map of the lasing emission wavelength at each pixel. Scale bars: 50 μm.

using the grating-based spectrometer and InGaAs camera running at high speed (50000 lines/s) to create a spectral map. Spectra that showed a characteristic, narrow lasing peak were then saved, and the wavelength of their lasing peaks identified (Figure 4b), thereby generating an association between individual cells and their LP emission wavelength barcode.

About 5000 HeLa cells tagged with an approximately equal number of rainbow LPs were plated in a single well of a 384-well plate. After successful cellular adhesion to the base of the plate, time-lapse imaging over a 24 h period was performed in which spectral maps and bright field images were recorded over a 3.3 mm × 3.3 mm × 12 μm volume (voxel size 1 μm × 1 μm × 4 μm) every 20 min. As cells moved, their paths were monitored by locating their internalized LP tags. LPs in adjacent frames were then matched by minimizing a modified Euclidean distance metric $\sqrt{(dx^2 + dy^2)/\Delta^2 + d\lambda^2/\delta\lambda^2}$ that accounted for both spatial distance traveled and lasing wavelength. Here, dx, dy, and $d\lambda$ represent the differences in x and y locations and wavelengths, respectively, and Δ = 100 pixels and $\delta\lambda$ = 1.5 nm are set as constants. This type of tracking metric, which was also used in our earlier work,[17] enables LPs to be identified and matched across multiple frames to create tracks that describe cell movements (Figures 5

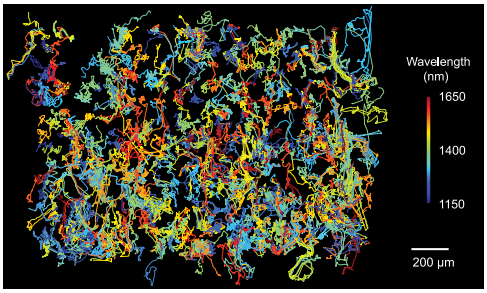

Figure 5. Cell tracking using rainbow LPs. Tracks of >1000 individual LPs over a 24 h period are shown over a subregion of the sample.

and S7). All cells in a given localized area were, with overwhelming probability, tagged uniquely, since the probability of nearby cells containing spectrally overlapping LPs was exceedingly low. This enabled faithful reconstruction of cellular movements. Note that the orientation of the LPs inside the cells is random and varies over time (Figure 4a), and therefore, the signal received may vary greatly from frame to frame. We discuss strategies to overcome this issue in Tang et al.[31]

DISCUSSION

We have demonstrated a straightforward fabrication technique enabling large quantities of microdisk LPs to be produced all from a single semiconductor wafer (~1.3 billion disk-lasers from a 3 in. wafer). The emission wavelengths can span a spectral range greater than that permitted by any single gain medium by several folds. Furthermore, stacking more layers increases the total number of microdisks produced from a single wafer. Specifically, if each column is comprised of m disk-producing layers arranged in a hexagonal array (the highest density pattern), the number of microdisk LPs produced per square cm of wafer is calculated to be ~$1.15 \times 10^8\ m/\alpha^2$, where α is the array pitch in microns (i.e., the center to center distance of adjacent columns). While our fabrication procedure has used α = 6 μm due to the limited resolution of our contact lithography tool, higher quality projection exposure systems could further decrease the spacing. As an alternative to photolithography, densely packed microspheres could be arranged on the wafer surface to form a hard etch mask.[26] This could theoretically enable α to approach the diameter of the disk. It should be possible to increase the number of layers to m > 9. Lattice-matched epitaxy as thick as several hundred microns has been demonstrated using techniques such as liquid-phase epitaxy.[34] However, the multilayered structure required to produce rainbow LPs must typically be grown by a technique such as MOCVD that can

https://doi.org/10.1021/acsphotonics.1c00343
ACS Photonics 2021, 8, 1301−1306

create sharply defined alternating layers. In practice, the accumulation of crystallographic faults, and the relatively slow rate of monocrystalline growth makes MOCVD growth of thicknesses much more than a few microns rare. In conclusion, the single-shot LP fabrication method demonstrated enables simple, low-cost, scalable fabrication, that will promote widespread use of LPs in life-science applications in which large numbers of colors are required.

■ ASSOCIATED CONTENT

Supporting Information

The Supporting Information is available free of charge at https://pubs.acs.org/doi/10.1021/acsphotonics.1c00343.

Epitaxial wafer design, additional rainbow LP fabrication illustrations, simulation results of microdisk resonances, micrographs of uncoated and coated LPs, additional cell tracking information, and silica coating details (PDF)

■ AUTHOR INFORMATION

Corresponding Author

Seok-Hyun Yun − *Wellman Center for Photomedicine, Massachusetts General Hospital, Boston, Massachusetts 02114, United States; Harvard Medical School, Boston, Massachusetts 02115, United States; Harvard-MIT Health Sciences and Technology, Massachusetts Institute of Technology, Cambridge, Massachusetts 02139, United States*; Email: syun@hms.harvard.edu

Authors

Paul H. Dannenberg − *Wellman Center for Photomedicine, Massachusetts General Hospital, Boston, Massachusetts 02114, United States; Harvard Medical School, Boston, Massachusetts 02115, United States; Harvard-MIT Health Sciences and Technology, Massachusetts Institute of Technology, Cambridge, Massachusetts 02139, United States*; orcid.org/0000-0002-9091-1611

Andreas C. Liapis − *Wellman Center for Photomedicine, Massachusetts General Hospital, Boston, Massachusetts 02114, United States; Harvard Medical School, Boston, Massachusetts 02115, United States*

Nicola Martino − *Wellman Center for Photomedicine, Massachusetts General Hospital, Boston, Massachusetts 02114, United States; Harvard Medical School, Boston, Massachusetts 02115, United States*

Jisoo Kang − *Wellman Center for Photomedicine, Massachusetts General Hospital, Boston, Massachusetts 02114, United States*

Yue Wu − *Wellman Center for Photomedicine, Massachusetts General Hospital, Boston, Massachusetts 02114, United States; Harvard Medical School, Boston, Massachusetts 02115, United States*; orcid.org/0000-0001-7680-9285

Anokhi Kashiparekh − *Wellman Center for Photomedicine, Massachusetts General Hospital, Boston, Massachusetts 02114, United States*

Complete contact information is available at: https://pubs.acs.org/10.1021/acsphotonics.1c00343

Author Contributions

‖These authors contributed equally to this work (P.H.D. and A.C.L.).

Notes

The authors declare the following competing financial interest(s): P.D. and S.-H.Y. hold patents licensed to LASE Innovation Inc., a company focused on commercializing technologies based on laser particles. S.-H.Y., A.C.L., and N.M. have financial interests in LASE Innovation Inc. that were reviewed and are managed by Massachusetts General Hospital and Partners HealthCare in accordance with their conflict of interest policies.

■ ACKNOWLEDGMENTS

This project was supported by the National Institutes Health (DP1- OD022296, P41-EB015903) and a MGH Research Scholar Award. This research used resources of the Center for Functional Nanomaterials, which is a U.S. DOE Office of Science Facility, at Brookhaven National Laboratory under Contract No. DE-SC0012704 and of the Harvard University's Center for Nanoscale Systems (CNS), a member of the National Nanotechnology Coordinated Infrastructure Network (NNCI), which is supported by the National Science Foundation under Award No. 1541959. N.M. acknowledges the Bullock postdoctoral fellowship.

■ REFERENCES

(1) Zhang, C.; Zou, C.-L.; Zhao, Y.; Dong, C.-H.; Wei, C.; Wang, H.; Liu, Y.; Guo, G.-C.; Yao, J.; Zhao, Y. S. Organic printed photonics: From microring lasers to integrated circuits. *Sci. Adv.* **2015**, *1*, e1500257.

(2) Wang, S.; Liu, Y.; Li, G.; Zhang, J.; Zhang, N.; Xiao, S.; Song, Q. Lead Halide Perovskite Based Microdisk Lasers for On-Chip Integrated Photonic Circuits. *Adv. Opt. Mater.* **2018**, *6*, 1701266.

(3) van Campenhout, J.; Rojo-Romeo, P.; Regreny, P.; Seassal, C.; Van Thourhout, D.; Verstuyft, S.; Di Cioccio, L.; Fedeli, J.-M.; Lagahe, C.; Baets, R. Electrically pumped InP-based microdisk lasers integrated with a nanophotonic silicon-on-insulator waveguide circuit. *Opt. Express* **2007**, *15*, 6744−6749.

(4) He, L.; Özdemir, Ş. K.; Zhu, J.; Kim, W.; Yang, L. Detecting single viruses and nanoparticles using whispering gallery microlasers. *Nat. Nanotechnol.* **2011**, *6*, 428−432.

(5) Wondimu, S.; Hippler, M.; Hussal, C.; Hofmann, A.; Krämmer, S.; Lahann, J.; Kalt, H.; Freude, W.; Koos, C. Robust label-free biosensing using microdisk laser arrays with on-chip references. *Opt. Express* **2018**, *26*, 3161−3173.

(6) Kim, H.-S.; Park, J.-M.; Ryu, J.-H.; Kim, S.-B.; Kim, C.-M.; Choi, Y.-W.; Oh, K.-R. Optical biochemical sensor based on half-circled microdisk laser diode. *Opt. Express* **2017**, *25*, 24939−24945.

(7) Fang, W.; Buchholz, D.; Bailey, R.; Hupp, J. T.; Chang, R. P.; Cao, H. Detection of chemical species using ultraviolet microdisk lasers. *Appl. Phys. Lett.* **2004**, *85*, 3666−3668.

(8) Foreman, M. R.; Swaim, J. D.; Vollmer, F. Whispering gallery mode sensors. *Adv. Opt. Photonics* **2015**, *7*, 168−240.

(9) Reynolds, T.; Riesen, N.; Meldrum, A.; Fan, X.; Hall, J. M.; Monro, T. M.; François, A. Fluorescent and lasing whispering gallery mode microresonators for sensing applications. *Laser Photonics Rev.* **2017**, *11*, 1600265.

(10) de Goede, M.; Chang, L.; Mu, J.; Dijkstra, M.; Obregón, R.; Martínez, E.; Padilla, L.; Mitjans, F.; Garcia-Blanco, S. M. Al 2 O 3: Yb 3+ integrated microdisk laser label-free biosensor. *Opt. Lett.* **2019**, *44*, 5937−5940.

(11) Zhang, Z.; Yang, L.; Liu, V.; Hong, T.; Vahala, K.; Scherer, A. Visible submicron microdisk lasers. *Appl. Phys. Lett.* **2007**, *90*, 111119.

(12) Ma, R.-M.; Oulton, R. F. Applications of nanolasers. *Nat. Nanotechnol.* **2019**, *14*, 12−22.

(13) McCall, S.; Levi, A.; Slusher, R.; Pearton, S.; Logan, R. Whispering-gallery mode microdisk lasers. *Appl. Phys. Lett.* **1992**, *60*, 289−291.

(14) Ning, C.-Z. Semiconductor nanolasers and the size-energy-efficiency challenge: a review. *Adv. Photonics* **2019**, *1*, 014002.
(15) Humar, M.; Hyun Yun, S. Intracellular microlasers. *Nat. Photonics* **2015**, *9*, 572−576.
(16) Schubert, M.; Steude, A.; Liehm, P.; Kronenberg, N. M.; Karl, M.; Campbell, E. C.; Powis, S. J.; Gather, M. C. Lasing within Live Cells Containing Intracellular Optical Microresonators for Barcode-Type Cell Tagging and Tracking. *Nano Lett.* **2015**, *15*, 5647−4652.
(17) Martino, N.; Kwok, S. J.; Liapis, A. C.; Forward, S.; Jang, H.; Kim, H.-M.; Wu, S. J.; Wu, J.; Dannenberg, P. H.; Jang, S.-J.; et al. Wavelength-encoded laser particles for massively multiplexed cell tagging. *Nat. Photonics* **2019**, *13*, 720−727.
(18) Schubert, M.; Woolfson, L.; Barnard, I. R.; Dorward, A. M.; Casement, B.; Morton, A.; Robertson, G. B.; Appleton, P. L.; Miles, G. B.; Tucker, C. S.; Pitt, S. J.; Gather, M. C. Monitoring contractility in cardiac tissue with cellular resolution using biointegrated microlasers. *Nat. Photonics* **2020**, *14*, 452−458.
(19) Feng, C.; Xu, Z.; Wang, X.; Yang, H.; Zheng, L.; Fu, H. Organic-nanowire-SiO2 core-shell microlasers with highly polarized and narrow emissions for biological imaging. *ACS Appl. Mater. Interfaces* **2017**, *9*, 7385−7391.
(20) Wu, X.; Chen, Q.; Xu, P.; Chen, Y.-C.; Wu, B.; Coleman, R. M.; Tong, L.; Fan, X. Nanowire lasers as intracellular probes. *Nanoscale* **2018**, *10*, 9729−9735.
(21) Fikouras, A. H.; Schubert, M.; Karl, M.; Kumar, J. D.; Powis, S. J.; Di Falco, A.; Gather, M. C. Non-obstructive intracellular nanolasers. *Nat. Commun.* **2018**, *9*, 1−7.
(22) Tien, M. C.; Ohta, A. T.; Yu, K.; Neale, S. L.; Wu, M. C. Heterogeneous integration of InGaAsP microdisk laser on a silicon platform using optofluidic assembly. *Appl. Phys. A: Mater. Sci. Process.* **2009**, *95*, 967−972.
(23) Koyama, F. Recent advances of VCSEL photonics. *J. Lightwave Technol.* **2006**, *24*, 4502−4513.
(24) Hsing, J. Y.; Tzeng, T. E.; Lay, T. S.; Shih, M. H. Vertically coupled double-microdisk lasers composed of InGaAs quantum dots-in-a-well active layers. *J. Appl. Phys. (Melville, NY, U. S.)* **2017**, *121*, 203107.
(25) Tu, X.; Wu, Y. K.; Guo, L. J. Vertically coupled photonic molecule laser. *Appl. Phys. Lett.* **2012**, *100*, 041103.
(26) Athanasiou, M.; Smith, R. M.; Pugh, J.; Gong, Y.; Cryan, M. J.; Wang, T. Monolithically multi-color lasing from an InGaN microdisk on a Si substrate. *Sci. Rep.* **2017**, *7*, 10086.
(27) Pran, S.; Runge, P. Revised refractive index and absorption of In $In_{1-x}Ga_xAs_yP_{1-y}$ lattice-matched to InP in transparent and absorption IR-region. *Opt. Mater. Exp.* **2016**, *6*, 251691.
(28) Ludowise, M. J. Metalorganic chemical vapor deposition of III-V semiconductors AR. *J. Appl. Phys. (Melville, NY, U. S.)* **1985**, *58*, 31.
(29) Dupuis, R. D.; Lynch, R. T.; Thurmond, C. D.; Bonner, W. A. Growth Of InP By Metalorganic Chemical Vapor Deposition (MOCVD). *Proc. SPIE* **1982**, 131−137.
(30) Adachi, S.; Noguchi, Y.; Kawaguchi, H. Chemical Etching of InGaAsP/InP DH Wafer. *J. Electrochem. Soc.* **1982**, *129*, 1053−1062.
(31) Tang, S.-J.; Dannenberg, P. H.; Liapis, A. C.; Martino, N.; Zhuo, Y.; Xiao, Y.-F.; Yun, S.-H. Laser particles with omnidirectional emission for cell tracking. *Light: Sci. Appl.* **2021**, *10*, 23.
(32) Patiño, T.; Soriano, J.; Barrios, L.; Ibáñez, E.; Nogués, C. Surface modification of microparticles causes differential uptake responses in normal and tumoral human breast epithelial cells. *Sci. Rep.* **2015**, *5*, 11371.
(33) Schubert, M.; Volckaert, K.; Karl, M.; Morton, A.; Liehm, P.; Miles, G. B.; Powis, S. J.; Gather, M. C. Lasing in live mitotic and non-phagocytic cells by efficient delivery of microresonators. *Sci. Rep.* **2017**, *7*, 40877.
(34) Mauk, M. G.; Tata, A. N.; Cox, J. A. Solution growth of thick III-V antimonide alloy epilayers (InAsSb, InGaSb, InGaAsSb, AlGaAsSb, and InAsSbP) for "virtual substrates. *J. Cryst. Growth* **2001**, *225*, 236−243.

https://doi.org/10.1021/acsphotonics.1c00343
ACS Photonics 2021, 8, 1301−1306